9 (2024) 100024

Contents lists available at ScienceDirect

IPEM-Translation

journal homepage: www.elsevier.com/locate/ipemt

Full Length Article

Photoplethysmogram-based heart rate and blood pressure estimation with hypertension classification

Aditta Chowdhury [a], Diba Das [a], Abdelrahman B.M. Eldaly [b], Ray C.C. Cheung [b], Mehdi Hasan Chowdhury [a,*]

[a] Department of Electrical and Electronic Engineering, Chittagong University of Engineering and Technology, Chittagong, Bangladesh
[b] Department of Electrical Engineering, City University of Hong Kong, Kowloon, Hong Kong

ARTICLE INFO

Keywords:
Blood pressure
FPGA
Heart rate
Hypertension
Photoplethysmogram

ABSTRACT

A photoplethysmogram (PPG) is an optically-derived signal that records the variation in blood volume within the microvasculature. Certain cardiovascular diseases (CVDs) are symptomatic of damaged blood vessels and problems in blood flow, including hypertension. While software implementations for heart rate and blood pressure estimation exist, point-of-care systems demand hardware-based implementations for real-time estimations to be useful for CVD detection. In this study, digital field programmable gate array (FPGA) based systems are developed for heart rate and blood pressure estimation from PPG signals by means of linear regression. In addition to the blood pressure estimation system, we present a prototype hypertension level detection system that achieves 92.42% accuracy while consuming 0.364 W of power. The Mean Absolute Error (MAE) ± Standard Deviation (SD) for heart rate estimation is 3.17 ± 2.79 beat per minute. The corresponding results for systolic and diastolic blood-pressure estimation are 4.75 ± 2.78 and 3.34 ± 2.60, respectively. The prototype can be further extended to wearable devices and medical equipment in the future.

1. Introduction

Blood pressure (BP) is a measure of the force of the blood against the arteries. Normal blood pressure is necessary to ensure the proper flow of blood from the heart to body organs and tissues. High BP is a risk factor for ischaemic heart disease and cardiovascular diseases [1]. Uncontrolled high BP can cause heart failure, kidney disease, dementia, and other health issues. High blood pressure affects more than 1 billion people worldwide and accounts for more than 20% of all cardiovascular diseases [2,3]. BP is categorized into systolic blood pressure (SBP) and diastolic blood pressure (DBP). Normal blood pressure level is generally considered if SBP<120 mm Hg and DBP<80 mm Hg [4]. If it exceeds a certain range, then it is called hypertension, which is a multifactorial disease involving a broad array of risk factors and targets different organ injuries and cardiovascular events [5]. Blood pressure is classified into different stages according to the level. Table 1 shows the different stages of hypertension and the corresponding blood pressures [6].

Both low and high BP can cause serious issues in the human body. Prolonged elevated blood pressure is a serious condition that may deteriorate if left untreated and lead to serious CVDs and ultimately to death. Among the blood pressure category of Table 1, Stage 1 and Stage 2 are considered as hypertension. Heart rate (HR) is also an essential parameter for physiological and pathological condition analysis. Detection of abnormal heart rate may indicate various disease states. The heart generally pumps the blood at about 60 to 100 beats per minute (bpm). An irregular heartbeat may indicate underlying different complications in the heart. Tachycardia is characterized by a heart rate exceeding 100 bpm and bradycardia by a heart rate below 60 bpm [7]. Reliable determination of heart rate can help detect the types of arrhythmia during emergency situations.

A non-invasive technique called photoplethysmography (PPG) measures volumetric fluctuations in blood circulation [8]. As the volume of blood changes with the pumping of blood from the heart, HR and BP can be estimated from the PPG signal. It is a simple technique that can be measured from the fingertip easily using a sensor. Hence, HR and BP prediction from PPG is simple and less time-consuming. Also, the feasibility of hypertension detection from PPG signal can also be analysed for quick identification and treatment.

Yue et al. [9] used a Support Vector Machine (SVM) method to predict blood pressure using 9 features from the PPG signal. Systolic pressure has a mean absolute error (MAE)+ standard deviation (SD) of 11.64 ± 8.20 mmHg and diastolic pressure has MAE + SD of 7.61 ± 6.78 mmHg. Hamed et al. [10] used 21 morphology features from the PPG

* Corresponding author.
E-mail address: mhchowdhury@cuet.ac.bd (M.H. Chowdhury).

https://doi.org/10.1016/j.ipemt.2024.100024
Received 7 September 2023; Received in revised form 13 March 2024; Accepted 13 March 2024
Available online 16 March 2024

Table 1
Blood Pressure Categories [6].

Blood pressure category	Systolic blood pressure (mm Hg)	Or	Diastolic blood pressure (mm Hg)
Low	<90	OR	<60
Normal	<120	And	<80
Prehypertension	120–139	Or	80-89
Stage 1 hypertension	140–159	Or	90-99
Stage 2 hypertension	> 160	Or	>100

signal of 30 patients for blood pressure estimation. They achieved an MAE of 3.32 mmHg for DBP and 7.41 mmHg for SBP. Mitja et al. [11] achieved an MAE of 8.57 mmHg for SBP and 4.42 mmHg for DBP. Examples of hardware-based implementations for BP estimation include real-time implementation of discrete circuit components such as microcontrollers, open-source hardware (e.g., Arduino), etc. Wang et al. [12] implemented a digital system for estimating blood pressure using a fast digital chip 3.97 mm^2 in size and having a power consumption of 15.62 mW. Their system achieved a maximum blood pressure error of ±6 mm Hg from PPG signals acquired from 8 patients. Bo et al. [13] designed a cuffless blood pressure prediction device utilizing ECG and PPG signals. Their system was implemented in heterogeneous digital signal processing and Digital Field Programmable Gate Array (FPGA) platforms, but it remains to be validated.

Research into the detection of hypertension from PPG signals is ongoing.

Graham et al. [14] achieved a maximum of 80% accuracy using a deep learning model for detecting hypertension from PPG signals. Erick et al. [15] applied different machine-learning algorithms to detect hypertension from PPG signals. They used 22 features and achieved an accuracy of 71.42% accuracy using an SVM classifier.

Heart rate prediction from PPG signals is also an active topic of research. Yuntong et al. [16] combined signal processing and machine learning and achieved 5% error in heart rate prediction. They used 10 to 20 features in their study for different trials. Attila et al. [17] used a convolution neural network for predicting heart rate. They obtained MAE of 7.47 bpm for the Wearable Stress and Affect Detection (WESAD) dataset [18] and an MAE of 7.65 bpm for the PPG-DaLiA dataset [19]. Xiangmao et al. [20] used deep learning to design a heart rate detection approach which achieved an average absolute error of 1.61 bpm. Motin et al. [21] achieved an MAE of 1.85 bpm for 23 PPG recordings during physical exercise. They used a Wiener filtering-based denoising algorithm to estimate heart rate. Karim et al. [22] designed an FPGA-based heart rate calculation system using a Xilinx system generator, though the accuracy and performance analysis of their designed system is missing.

The above analysis validates the use of PPG signals for blood pressure and heart rate estimation. However, most of the research works done for these parameter estimations and hypertension detection is at the software level. While there are a few reports of hardware-based implementations using FPGA or predecessors in the literature [12,13,22], they lack system performance and power analyses; also, the number of subjects taking part in those studies is not adequate for proper validation. The present study reports on the hardware developments in order for a point-of-care system to be used for patient assessment in the clinical setting.

2. Materials and methods

To construct a system for predicting blood pressure and heart rate, we must choose an appropriate dataset that includes the PPG signal in addition to the participant's blood pressure and heart rates. After denoising, selected features were extracted from the signal and used to develop a robust classifier model for estimating blood pressure and heart rate. Thereafter, the system was modified to allow for hypertension detection. Finally, the performance of the system was analysed. The overall methodology is depicted in Fig. 1

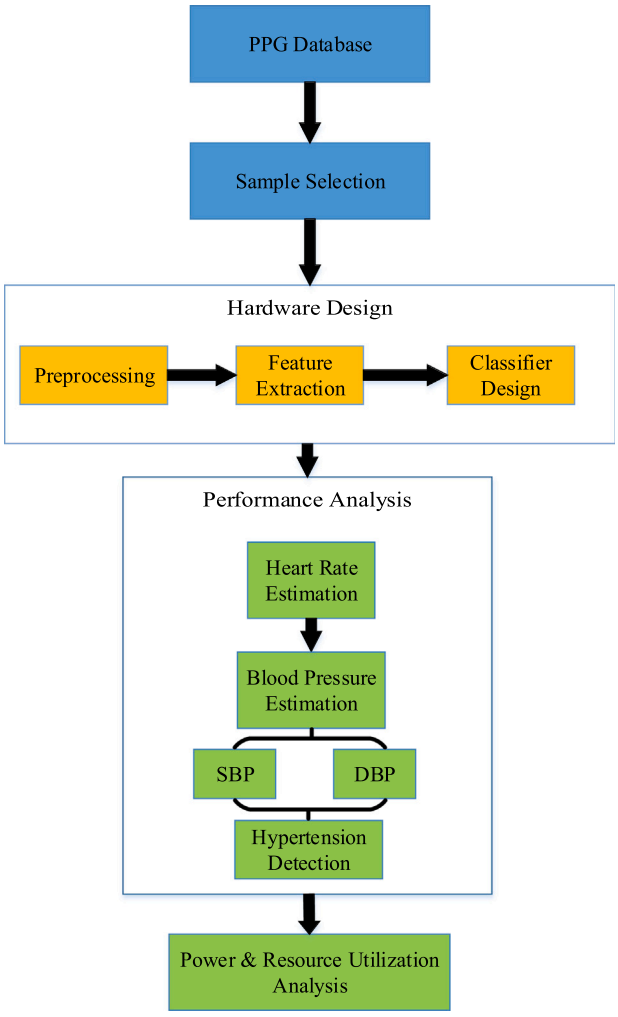

Fig. 1. Overall methodology of the study.

2.1. Dataset and data selection

The open-source dataset "PPG-BP" provided the signals on which the present study is based [23]. A total of 219 subjects participated in the data acquisition procedure where 3 segments of PPG signal were collected. Each segment contains 2100 samples and the sampling rate is 1 KHz. The data set contains the age, sex, height, systolic and diastolic blood pressure and heart rate of each subject. Also, the Signal Quality Index (SQI) for each recording is included in the dataset. A symmetric signal's probability distribution is measured by skewness, which has been found to be connected to the quality of the PPG waveform [24].

Only signals having SQI equal to or above 0.8 were selected for analysis as signals having higher SQI are known to provide better accuracy and estimation [25], which yielded 331 recordings from 153 subjects. After estimating both the systolic and diastolic blood pressures, we designed a hypertension classification system. Out of the total selected recordings, 80% were used for training while the remainder were used in testing.

2.2. Hardware platform

Hardware-based digital and embedded systems are becoming more common due to their multifunction capability along with low cost and high-performance accuracy [26]. FPGAs, Complex Programmable Logic Devices (CPLDs), Simple Programmable Logic Devices (SPLDs),

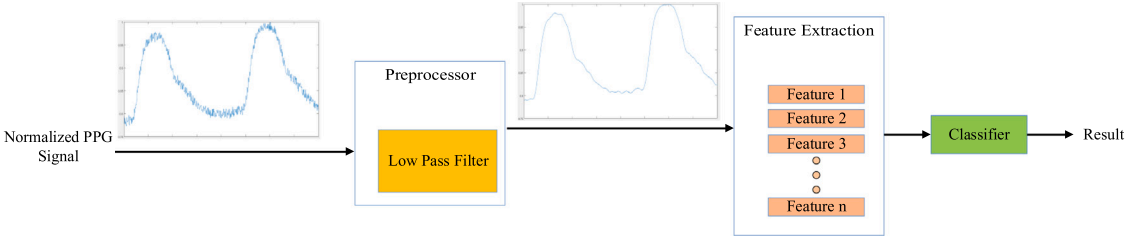

Fig. 2. Overall hardware structure for hypertension detection and heart rate, blood pressure estimation.

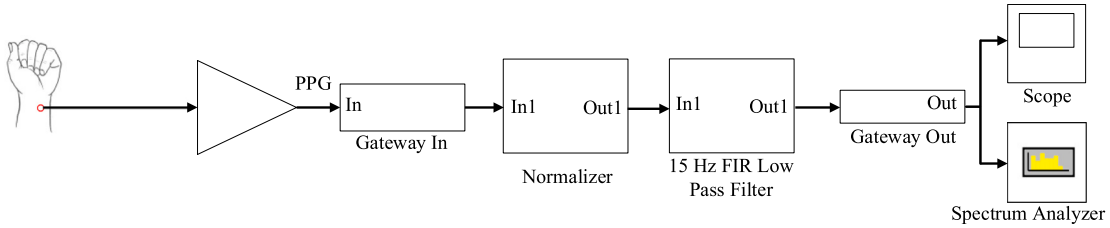

Fig. 3. Preprocessing subsystem for denoising raw PPG signals.

microcontrollers, etc., are available for hardware-based digital system design and implementation. Hard-wired analogue circuit design is another option, but it is more complex and requires a large number of components; moreover, noise, nonlinearities, and distortion affect the performance of the analogue circuits. While FPGAs contain much more logic blocks than CPLD or SPLD, they allow for greater customization and more complex processes than microcontrollers. Moreover, they can perform an operation with fewer resources than an analogue circuit, occupying less board space while exhibiting greater power efficiency and reliability.

We used a Xilinx system generator (XSG, Xilinx, Inc., San Jose, CA, USA) and MATLAB® (The Mathworks, Inc., Natick, Massachusetts, USA) to design the proposed system. In XSG we utilized a ZedBoardTM AMD Zynq-7000 ARM/FPGA Development Board to realize the concept of the study. It offers the advantage of low cost and long life. First, we have to design the preprocessing subsystem, feature extraction subsystem, and classifier subsystem in the XSG and then analyse the performance of the developed prototype. The overall hardware architecture is shown in Fig. 2.

2.3. Preprocessing

PPG signals may be contaminated by motion artifacts, muscle noise, baseline wander, etc., during data acquisition, and need to be processed before further analysis. Before preprocessing, the PPG signal is normalized using a divider block. Then the noise signals outside the range of PPG signal have to be suppressed. To eliminate the high-frequency noise, a low pass filter of 15 Hz needs to be developed.

Finite impulse response (FIR) filters were designed as low-pass filters for our system. FIR filters are stable due to their non-feedback nature and also provide advantages of phase linearity and low coefficient sensitivity over infinite impulse response (IIR) filter [27]. The Xilinx system generator provides a Filter Design and Analysis (FDA) tool that allows users to design the filter according to their specifications. The filter order for the low pass filter in this case was 81. The fast Fourier transform (FFT) of the preprocessed signal was checked to ensure the denoising of the signal was adequate. The preprocessor subsystem of Fig. 2 is expanded in Fig. 3.

2.4. Feature extraction

In order to build a simple hardware architecture, the features must be chosen such that they can be extracted from the hardware prototype. Statistical features are relatively easy to implement in the XSG. We extracted the following statistical features when designing the hardware-based system: sum, mean, absolute energy (AE), root mean square (RMS), variance, standard deviation, skewness and kurtosis. Applying the various combinations of these features, it was found that the combination of mean, variance, absolute energy, and root mean square provided the best results. We chose these four statistical features since they have been found to be important features of PPG in other studies based on the same dataset [8,28,29].

The mean, x, is expressed by:

$$mean, \bar{x} = \frac{1}{N}\sum_{i=1}^{N} x_i \tag{1}$$

The variance is defined as follows:

$$Variance, \sigma^2 = \frac{\sum_{i=1}^{N}(x_i - \bar{x})^2}{N} \tag{2}$$

Absolute signal energy (AE) is a measure of strength of the data that can be derived from the equation:

$$AE = \sum_{i=1}^{N} x_i^2 \tag{3}$$

The root mean square value can be found from the following equation:

$$RMS = \sqrt{\frac{1}{N}\sum_{i=1}^{N} x_i^2} \tag{4}$$

In Eqs. (1)–(4), N is the total number of samples and x_i is the value of i_{th} sample of a signal. These equations are implemented in the hardware design in XSG.

The preprocessed signal is stored in a RAM first, as shown in Fig. 4. It uses two counters and a multiplexer (Mux) for storing each sample in a data address. The first counter counts up to 2100 and till then, the writing enable (WE) is disabled using a not gate. The counter 2 starts counting with counter 1, but it enables the writing enable of RAM after counting 2100 and continues to count till 4200 for storing each sample. Two comparator blocks are used to generate two control signals: ctrl_1(i) and ctrl_2(i). They are used to store values in the register during feature extraction.

The system architecture of the different feature extractor designs in XSG is presented in Fig. 5. For mean extraction, an accumulator adds all the samples of a PPG signal. The output of the accumulator is divided by the total no. of sample to extract mean value and it is stored in a

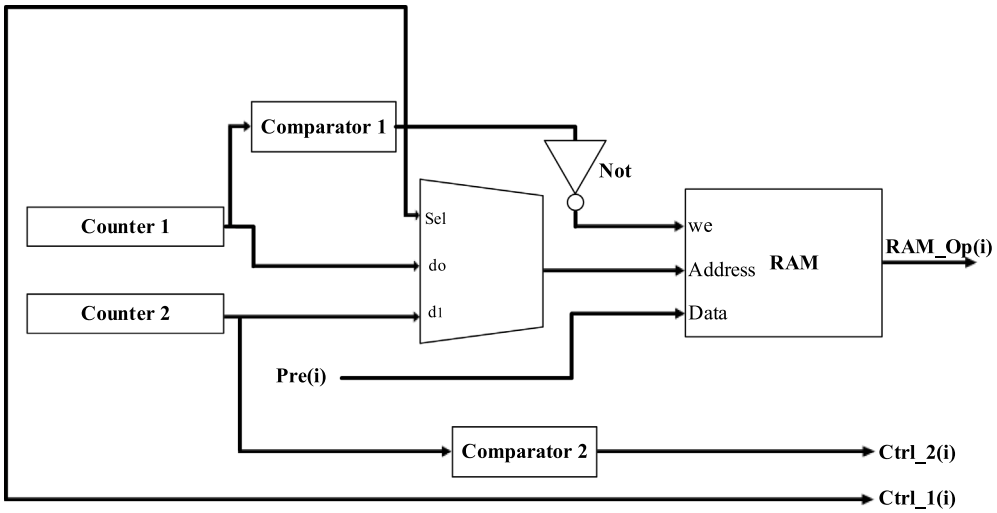

Fig. 4. Memory and control subsystem for feature extraction.

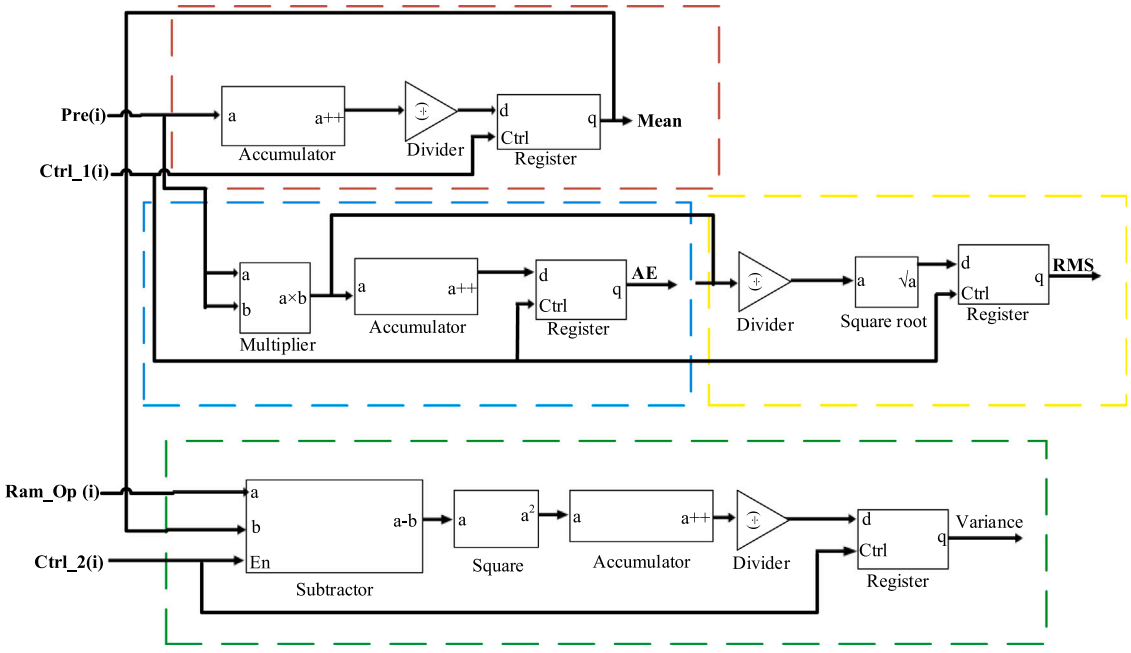

Fig. 5. Feature extraction subsystem.

register. In the case of AE, the sample is squared using a multiplier block and then added using an accumulator. In the case of RMS, the output of the accumulator used in AE is divided by the total no. of samples and then root squaring the output of the divider block, we get the desired result. Ctrl_1(i) is used to store the values in registers.

For variance determination, we have used a subtractor block, which subtracts the mean value from the sample stored in the RAM. It is squared and an accumulator is used for summation, which is divided by the total number of samples to get the variance. Ctrl_2(i) is used to store the value in a register.

2.5. Classifier selection

Various machine-learning algorithms are available for the classification of PPG signals. For hardware implementation, however, one needs to select a hardware-friendly classifier and also be able to utilize the extracted features simply. Accordingly, linear regression was used in this study as it is simple to implement at the hardware level, requiring fewer resources that will ensure lower power consumption. For estimating or predicting a variable, regression analysis is usually used [30]. In mathematical analysis, linear regression is employed when we want to measure the expected effects and the modelling of those effects against one or more input variables [31]. Simple linear regression and multiple linear regression are two different types of linear regression. As we had extracted a total of 4 statistical features for our study, we used multiple linear regression to design the model. In multiple linear regression, there is more than one independent variable on which the estimated value depends. It is expressed by the following:

$$y = b_o + b_1 x_1 + b_2 x_2 + \cdots + b_m x_m \tag{5}$$

where y is the estimated value, b_o is the intercept, $b_1, b_2, \ldots, b_m$ are regression coefficient, and $x_1, x_2, x_3, \ldots, x_m$ are the independent variables or the feature values.

The system architecture designed in Xilinx is shown in Fig. 6. The regression coefficient and the intercept values were taken from the

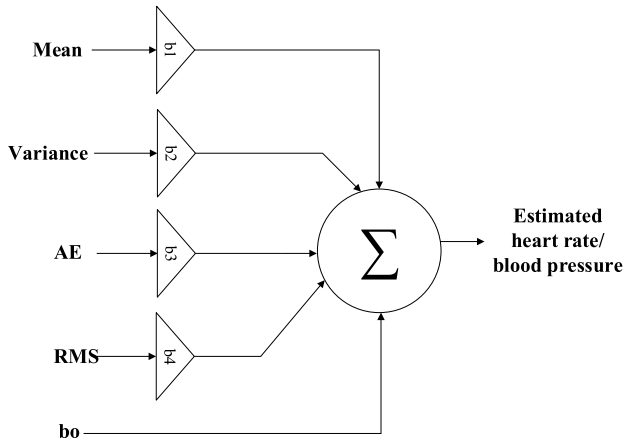

Fig. 6. Classifier subsystem for heart rate and blood pressure detection.

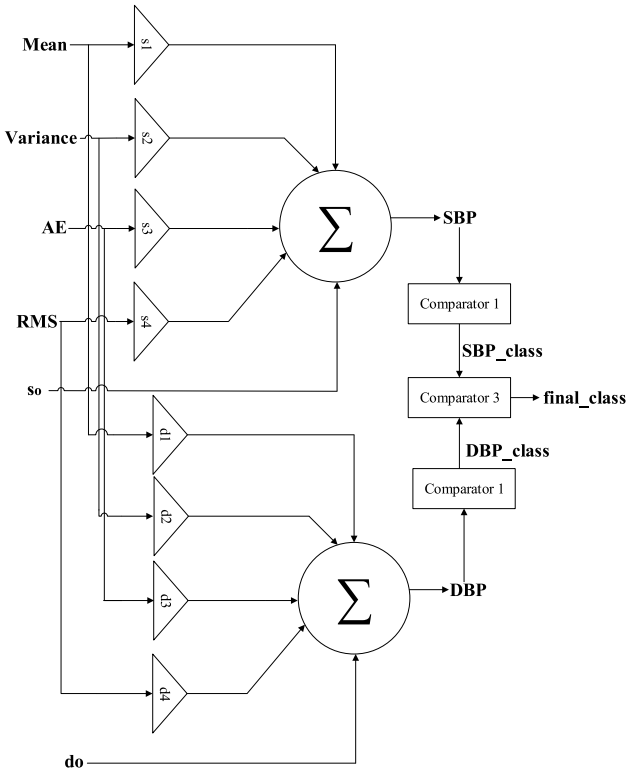

Fig. 7. Hardware architecture for hypertension classification.

model trained in MATLAB. This system estimated heart rate, systolic blood pressure and diastolic blood pressure from the PPG signal.

For developing the hypertension classification system, the estimated SBP and DBP were utilized. In this system, the extracted statistical features went to two linear regression models, which estimated the SBP and DBP simultaneously. The SBP and DBP values were checked by two individual comparators, which diagnosed the hypertension levels of SBP and DBP, respectively. The hardware architecture is shown in Fig. 7. Hypertension is classified into 5 levels for this study. Class 1 indicates Stage 2 hypertension, Class 2 indicates Stage 1 hypertension, Class 3 indicates prehypertension, Class 4 indicates low blood pressure and Class 5 indicates normal. The final comparator in the hypertension classification system compares the two comparator outputs and shows the hypertension level according to the hypertension classification as shown in Table 1.

Table 2
Pearson correlation coefficient for hardware and simulation-based Features.

Feature	Pearson correlation coefficient
Mean	0.9982
Variance	0.9882
AE	0.9914
RMS	0.9795

3. Performance analysis

3.1. Performance of preprocessor

We have designed the preprocessor with a low-pass filter. The FFT of the raw PPG signal and output of the preprocessor is shown in Fig. 8. It can be seen that the noise is almost fully suppressed above 15 Hz.

3.2. Performance of feature extractor

The feature extractor subsystem extracts four statistical features. To verify the extracted features, they are compared with features extracted in MATLAB. We determined the Pearson correlation coefficient and root-squared error(RSE) values for statistical analysis.

The most popular method for determining a linear connection is the Pearson correlation coefficient (r). It is expressed by the following equation:

$$r = \frac{1}{n-1}\left(\frac{\sum x \sum y(x-\bar{x})(y-\bar{y})}{S_x S_y}\right) \tag{6}$$

where r is Pearson correlation coefficient, n is the total number of compared data, $\bar{x}$ and $\bar{y}$ are the average of x and y values, x values are considered software data and y values are considered hardware data, S_x&S_y are corresponding standard deviations.

In our study, we used four statistical features, which are extracted from the designed subsystem. The Pearson correlation coefficients of these features are presented in Table 2. A Pearson correlation coefficient value close to 1 indicates higher accuracy. From the table, we can see all the extracted statistical features from the subsystem have a Pearson correlation coefficient above 0.97.

Another metric is root squared error (RSE), one of the common methods for gauging how well a model predicts quantitative data. It is expressed by:

$$RSE = \sqrt{(X-Y)^2} \tag{7}$$

where X represents software outcome and Y represents hardware outcome. RSE Value closer to 0 indicates higher accuracy [32]. Fig. 9 shows the boxplot of RSE data for the extracted features. A closer value to 0 indicates higher accuracy. In the figure, all the RSE data are close to 0.

The statistical feature values extracted from hardware have variations with the features extracted from software. In the hardware design, we had to convert the data type of the signals several times. Due to the conversion between different datatypes and computational delays, there are slight mismatches between hardware and software features. However, the Pearson correlation coefficient closer to 1 and RSE values closer to 0 give a satisfactory result.

3.3. Performance of the classifier

We have designed a system to estimate the heart rate and blood pressure from the PPG signals. The model adds the product of feature values with their correlated regression coefficients and finally, the intercept value is added to provide the final result. The heart rate value ranges from 52 to 103 bpm, systolic pressure ranges from 80 to 181 mmHg and diastolic pressure ranges from 42 to 102 mmHg. Among the

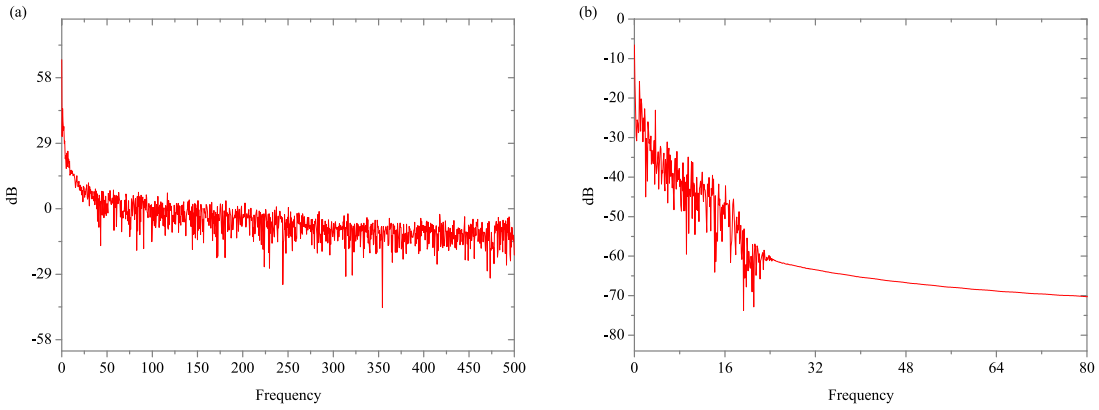

Fig. 8. FFT response of (a) raw PPG signal, (b) filtered signal.

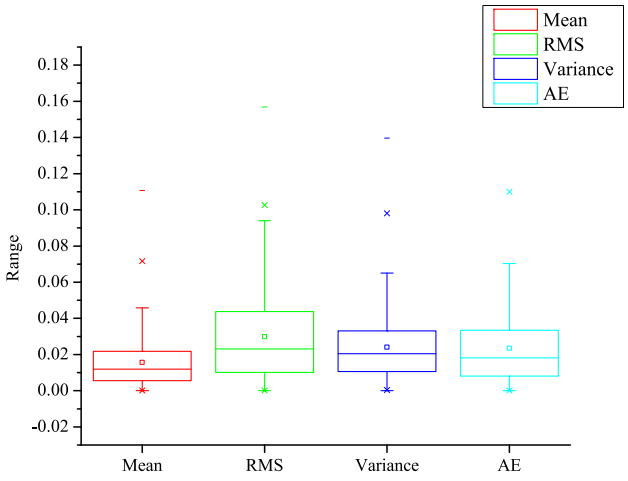

Fig. 9. Boxplot of RSE for different features.

Table 3
Resource utilization analysis of the developed prototypes.

Resource	Available	HR & BP estimation	Hypertension classification
		Utilization	Utilization
LUT	53 200	9407	11 222
LUTRAM	17 400	330	330
FF	106 400	2062	2444
BRAM	140	7.50	7.50
DSP	220	65	77
IO	200	65	47
BUFG	32	1	1

Table 4
Comparison of our hypertension detection system with previous works.

Reference	Features	Implementation level	Method	Accuracy
Frederick et al. [14]	–	Software	CNN	80.00%
Martinez-Ríos et al. [15]	22	Software	SVM	71.42%
Sadad et al. [33]	30	Software	Decision tree	99.50%
Evdochim et al. [34]	4	Software	Quadratic SVM	72.90%
Present study	4	Hardware	Linear regression	92.42%

331 segments, we have randomly selected 80% for training and 20% segments for testing purposes as we mentioned before.

The system predicts heart rate to be within 4.3%, that is, the mean absolute error + standard deviation is 3.17 ± 2.79 beat per minute. In terms of blood pressure, the corresponding figures are systolic blood pressure to within 3.73% of the true values and diastolic blood pressure to within 4.6% of the actual values. The MAE+SD for systolic and diastolic blood pressure are 4.75 ± 2.78 and 3.34 ± 2.6, respectively. The Bland–Altman plot for systolic blood pressure, diastolic blood pressure and heart rate is shown in Fig. 10. When two separate measurement methods have differing measurements, the differences can be seen visually via a Bland–Altman plot. It is frequently used to evaluate how well a new measurement tool or method compares to an existing tool or method of measurement. It can be seen from the figure that for values that are too high or low, the estimated values have higher differences from the actual values. But the deviation is mostly within 5% for SBP of 89 to 164 mmHg, DBP of 48 to 94 mmHg and heart rate of 60 to 92 bpm. The modified classifier for detecting hypertension was tested and it correctly predicted the hypertension level of 61 PPG recordings out of 66 PPG signals selected randomly. It predicted correctly the hypertension level with an overall accuracy of 92.42%.

3.4. Resource and power analysis

The Xilinx ZedBoard utilizes Lookup Table (LUT), Lookup Table Random Access Memory (LUTRAM), Block Random Access Memory (BRAM), Input/Output (IO), Flipflop (FF), etc., to process the signal and provide the output. The resource utilization for the designed prototype is shown in Table 3.

The heart rate and blood pressure prediction system requires slightly fewer resources than the other one. The use of LUTRAM, BRAM, and Global Buffer (BUFG) are the same for both prototypes. The hypertension classification system requires more LUT, FF and DSP for functioning. The resource utilization proves the efficacy of ZedBoard Zynq for implementing our design in this FPGA.

Fig. 11 depicts the power utilization analysis of the heart rate and blood pressure detection system. As the system requires fewer resources, the total power consumption is lower for this system than for the other system. The system requires maximum power for static operation. The signal and logic blocks consume maximum power for dynamic operation. The system requires a total of 0.338 W of power, among which 0.108 W is for static operation and 0.230 W is for dynamic operation.

The power utilization of the hypertension classification system is shown in Fig. 12. The static power consumption is almost the same as the previous design, being 0.109 W. The system consumes maximum power for signal and logic operation. A power requirement of 0.255 W for dynamic operation makes the total power consumption of the system 0.364 W. The power utilization analysis proves our system to be power efficient, consuming much less than even 0.4 W.

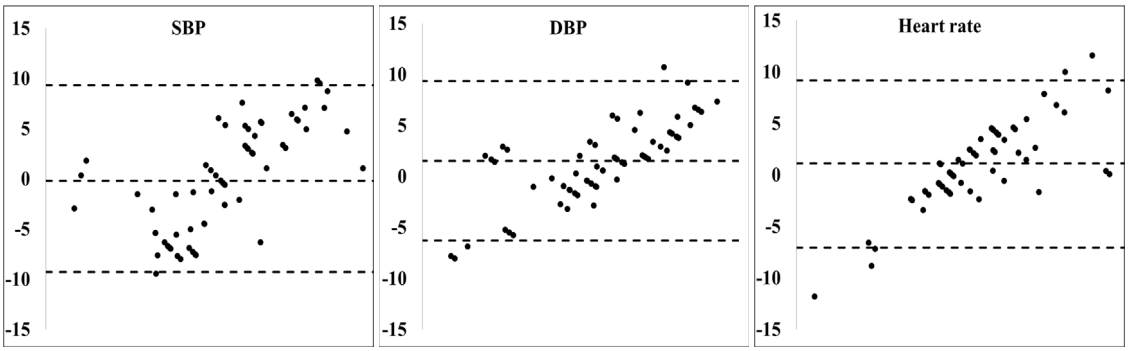

Fig. 10. Bland–Altman plot for SBP, DBP and HR estimation.

Table 5
Comparison study of heart rate estimation.

Reference	Subjects	Implementation level	Method	MAE	SD	Error rate
Zhang et al. [16]	12	Software	Signal processing & ML	–	–	5.00%
Reiss et al. [17]	15	Software	CNN	7.65 bpm	–	–
Chang et al. [20]	12 recordings	Software	DCNN	1.61 bpm	–	–
Motin et al. [21]	23 recordings	Software	Weiner filtering	1.85 bpm	–	–
Islam et al. [35]	12	Software	Time–frequency domain approach	1.16 bpm	±1.74	–
Present study	153	Hardware	Linear Regression	3.17 bpm	±2.79	4.30%

Table 6
Comparison study of blood pressure estimation.

Reference	Subjects	Features	Implementation level	Method	SBP (mmHg)			DBP (mmHg)		
					MAE	SD	Error	MAE	SD	Error
Zhang et al. [9]	19	9	Software	SVM	11.64	±8.20	–	7.61	±6.78	–
Samimi et al. [10]	30	21	Software	ANN	7.41	10.40	–	3.32	4.89	–
Slapničar et al. [11]	41	13	Software	Regression	8.57	–	–	4.42	–	–
Kurylyak et al. [36]	–	21	Software	ANN	3.80	±3.46	–	2.21	±2.09	–
Schlesinger et al. [37]	–	–	Software	CNN	5.95	–	–	3.41	–	–
Present study	153	4	Hardware	Linear Regression	4.75	±2.78	3.73%	3.34	±2.60	4.60%

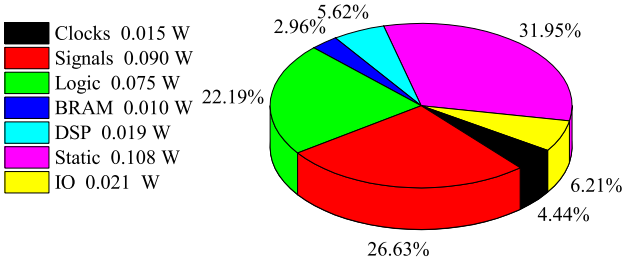

Fig. 11. Power Utilization for HR and BP estimation.

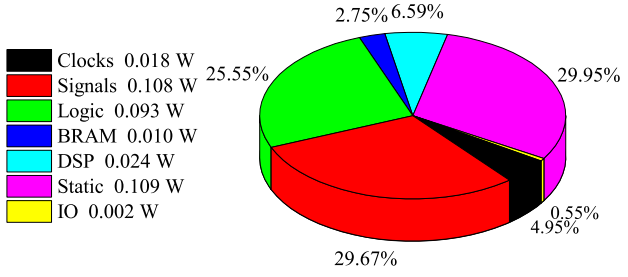

Fig. 12. Power Utilization for hypertension classification.

3.5. Comparative study

There are some works on hypertension detection from PPG signals. Their key performances are shown in Table 4. It can be seen that previous works are mostly done at the software level. Though our implemented prototype is designed at the hardware level, it surpluses most software-based works with an accuracy of 92.42%. Previous works used mostly waveform features, while this study has utilized statistical features. Also, our system uses fewer features than most of the previous works.

Analysis of previous works on heart rate detection from PPG signal is presented in Table 5. Also, Table 6 shows the comparative study with previous works on blood pressure estimation from PPG. From Tables 5 and 6, we can see most of the works have been done at the software level. Although the systems developed by Wang et al. [12] and Meddah et al. [22] are based on FPGA, the system performance analysis is missing in those studies. Furthermore, most works considered few subjects or recordings for their study. Our study considered a total of 331 PPG recordings from 153 subjects for heart rate and blood pressure prediction. Our hardware prototype outperforms most of the previous works regarding mean absolute error or prediction accuracy level, even though they are software-based. Also, power and resource consumption analysis prove the efficacy of our system.

4. Conclusions

Here, we present an FPGA-based hypertension detection and heart rate and blood pressure estimation system. The hardware-based design was implemented on a Xilinx system generator platform. The ZedBoard Zynq-7000 ARM/FPGA Development Board we used as the demonstrator was found to provide sufficient logical and signal processing resources required for each system. The power consumption study demonstrated the efficiency of the systems as a power-efficient device. For developing the FPGA-based system, the preprocessor stage was designed with a low-pass filter and the FFT of the preprocessor indicated

the removal of undesired noises. Then the feature extraction subsystem extracted 4 statistical features that were hardware-friendly. Linear regression was used for the classifier design to predict heart rate and blood pressure. The SBP and DBP estimation systems were combined and extended using three comparators to classify the hypertension detection system. The system detected hypertension with an accuracy of 92.4% and estimated heart rate and blood pressure to within 5% of actual values in a certain range, which is significant for a cuffless, non-invasive measurement system. Although previous studies have reported better performance at the software level, the present hardware-based system achieved satisfactory results using fewer features and involving more subjects. And while the system has the potential to extract additional features, the static power consumption is considered too high and further work will be needed to improve the performance. Nevertheless, there is scope for extending the systems to other applications, including point-of-care systems, wearable devices and medical equipment.

Declaration of competing interest

The authors declare that they have no known competing financial interests or personal relationships that could have appeared to influence the work reported in this paper.

Acknowledgement

The CityU Architecture Lab for Arithmetic and Security (CALAS), City University of Hong Kong, Kowloon, Hong Kong has supported for the implementation of this work.

Funding

The authors have no relevant financial or non-financial interests to disclose.

References

[1] B. Zhou, P. Perel, G.A. Mensah, M. Ezzati, Global epidemiology, health burden and effective interventions for elevated blood pressure and hypertension, Nat. Rev. Cardiol. 18 (11) (2021) 785–802, http://dx.doi.org/10.1038/s41569-021-00559-8.

[2] M.H. Forouzanfar, et al., Global burden of hypertension and systolic blood pressure of at least 110 to 115mmHg, 1990–2015, JAMA - J. Am. Med. Assoc. 317 (2) (2017) 165–182, http://dx.doi.org/10.1001/jama.2016.19043.

[3] S. Yusuf, et al., Modifiable risk factors, cardiovascular disease, and mortality in 155722 individuals from 21 high-income, middle-income, and low-income countries (PURE): a prospective cohort study, Lancet 395 (10226) (2020) 795–808, http://dx.doi.org/10.1016/S0140-6736(19)32008-2.

[4] S.T. Hardy, S. Sakhuja, B.C. Jaeger, S. Oparil, O.P. Akinyelure, T.M. Spruill, J. Kalinowski, M. Butler, D.E. Anstey, T. Elfassy, G.S. Tajeu, N.B. Allen, O. Reges, M. Sims, D. Shimbo, P. Muntner, Maintaining normal blood pressure across the life course: The JHS, Hypertension 77 (5) (2021) 1490–1499, http://dx.doi.org/10.1161/HYPERTENSIONAHA.120.16278.

[5] O. Reges, A.E. Krefman, S.T. Hardy, Y. Yano, P. Muntner, D.M. Lloyd-Jones, N.B. Allen, Decision tree-based classification for maintaining normal blood pressure throughout early adulthood and middle age: Findings from the coronary artery risk development in Young adults (CARDIA) study, Am. J. Hypertens. 34 (10) (2021) 1037–1041, http://dx.doi.org/10.1093/ajh/hpab099.

[6] G.L. Schwartz, S.G. Sheps, A review of the sixth report of the joint national committee on prevention, detection, evaluation, and treatment of high blood pressure, Curr. Opin. Cardiol. 14 (2) (1999) 161–168, http://dx.doi.org/10.1097/00001573-199903000-00014.

[7] P. Kansara, R. Dhar, R. Shah, D. Mehta, P. Raut, Heart rate measurement, J. Phys. Conf. Ser. 1831 (1) (2021) http://dx.doi.org/10.1088/1742-6596/1831/1/012020.

[8] A. Chowdhury, D. Das, K. Hasan, R.C.C. Cheung, M.H. Chowdhury, An FPGA implementation of multiclass disease detection from PPG, IEEE Sens. Lett. 7 (11) (2023) 1–4, http://dx.doi.org/10.1109/LSENS.2023.3322288.

[9] Y. Zhang, Z. Feng, A SVM method for continuous blood pressure estimation from a PPG signal, in: ACM International Conference Proceeding Series, Part F1283, 2017, pp. 128–132, http://dx.doi.org/10.1145/3055635.3056634.

[10] H. Samimi, H.R. Dajani, A PPG-based calibration-free cuffless blood pressure estimation method using cardiovascular dynamics, Sensors 23 (8) (2023) http://dx.doi.org/10.3390/s23084145.

[11] G. Slapničar, M. Luštrek, M. Marinko, Continuous blood pressure estimation from PPG signal, Informatica (Slovenia) 42 (1) (2018) 33–42.

[12] J.H. Wang, M.H. Yeh, P.C. Chao, T.Y. Tu, Y.H. Kao, R. Pandey, A fast digital chip implementing a real-time noise-resistant algorithm for estimating blood pressure using a non-invasive, cuffless PPG sensor, Microsyst. Technol. 26 (11) (2020) 3501–3516, http://dx.doi.org/10.1007/s00542-020-04946-y.

[13] B. Liang, K. Duan, Q. Xie, M. Atef, Z. Qian, G. Wang, Y. Lian, Live demonstration: A support vector machine based hardware platform for blood pressure prediction, in: Proceedings - 2016 IEEE Biomedical Circuits and Systems Conference, BioCAS 2016, Vol. 7, 2016, p. 130, http://dx.doi.org/10.1109/BioCAS.2016.7833744.

[14] G. Frederick, et al., PPG signals for hypertension diagnosis: A novel method using deep learning models, 2023, arXiv preprint arXiv:2304.06952.

[15] E. Martinez-Ríos, L. Montesinos, M. Alfaro-Ponce, A machine learning approach for hypertension detection based on photoplethysmography and clinical data, Comput. Biol. Med. 145 (January) (2022) 105479, http://dx.doi.org/10.1016/j.compbiomed.2022.105479.

[16] Y. Zhang, J. Xu, M. Xie, W. Wang, K. Ye, J. Wang, D. Zhu, PPG-based heart rate estimation with efficient sensor sampling and learning models, in: 18th IEEE International Conference on Embedded Software and Systems (ICESS), 2022, pp. 1971–1978, http://dx.doi.org/10.1109/HPCC-DSS-SmartCity-DependSys57074.2022.00294, arXiv:2303.13636.

[17] A. Reiss, I. Indlekofer, P. Schmidt, K. Van Laerhoven, Deep PPG: Large-scale heart rate estimation with convolutional neural networks, Sensors (Switzerland) 19 (14) (2019) 1–27, http://dx.doi.org/10.3390/s19143079.

[18] S. Philip, R. Attila, D. Robert, M. Claus, V. Kristof, Introducing WESAD, a multimodal dataset for Wearable Stress and Affect Detection, ICMI, Boulder, USA, 2018.

[19] A. Reiss, I. Indlekofer, P. Schmidt, PPG-DaLiA, 2019, http://dx.doi.org/10.24432/C53890, UCI Machine Learning Repository.

[20] X. Chang, G. Li, G. Xing, K. Zhu, L. Tu, DeepHeart: A deep learning approach for accurate heart rate estimation from PPG signals, ACM Trans. Sensor Netw. 17 (2) (2021) 1–18, http://dx.doi.org/10.1145/3441626.

[21] M.A. Motin, C.K. Karmakar, M. Palaniswami, PPG derived heart rate estimation during intensive physical exercise, IEEE Access 7 (c) (2019) 56062–56069, http://dx.doi.org/10.1109/ACCESS.2019.2913148.

[22] K. Meddah, M. Kedir-Talha, H. Zairi, FPGA-based system for heart rate calculation based on PPG signal, in: 2017 5th International Conference on Electrical Engineering - Boumerdes, ICEE-B 2017, January, 2017, pp. 1–5, http://dx.doi.org/10.1109/ICEE-B.2017.8192157.

[23] Y. Liang, Z. Chen, G. Liu, M. Elgendi, A new, short-recorded photoplethysmogram dataset for blood pressure monitoring in China, Sci. Data 5 (2018) 1–7, http://dx.doi.org/10.1038/sdata.2018.20.

[24] R. Krishnan, B. Natarajan, S. Warren, Two-stage approach for detection and reduction of motion artifacts in photoplethysmographic data, IEEE Trans. Biomed. Eng. 57 (8) (2010) 1867–1876, http://dx.doi.org/10.1109/TBME.2009.2039568.

[25] S.H. Liu, R.X. Li, J.J. Wang, W. Chen, C.H. Su, Classification of photoplethysmographic signal quality with deep convolution neural networks for accurate measurement of cardiac stroke volume, Appl. Sci. (Switzerland) 10 (13) (2020) http://dx.doi.org/10.3390/app10134612.

[26] G. Dere, Biomedical applications with using embedded systems, in: Data Acquisition-Recent Advances and Applications in Biomedical Engineering, IntechOpen, 2021, http://dx.doi.org/10.5772/intechopen.96070.

[27] A. Chandra, S. Chattopadhyay, Design of hardware efficient FIR filter: A review of the state-of-the-art approaches, Eng. Sci. Technol., Int. J. 19 (1) (2016) 212–226, http://dx.doi.org/10.1016/j.jestch.2015.06.006.

[28] M.S. Zaman, B.I. Morshed, Generalization of data reliability metric (DReM) mechanism for pulsatile bio-signals, in: IEEE International Conference on Electro Information Technology, 2021-May, IEEE, 2021, pp. 282–286, http://dx.doi.org/10.1109/EIT51626.2021.9491839.

[29] F. Farjana, S.K. Singha, A.A. Farabi, Cuffless blood pressure determination using photoplethysmogram (PPG) signal based on multiple linear regression analysis, in: 2021 International Conference on Science and Contemporary Technologies, ICSCT 2021, IEEE, 2021, http://dx.doi.org/10.1109/ICSCT53883.2021.9642626.

[30] C. Limpabandhu, F.S.W. Hooper, R. Li, Z. Tse, Regression model for predicting core body temperature in infrared thermal mass screening, IPEM-Translation 3–4 (March) (2022) 100006, http://dx.doi.org/10.1016/j.ipemt.2022.100006.

[31] H.-I. Lim, A linear regression approach to modeling software characteristics for classifying similar software, in: 2019 IEEE 43rd Annual Computer Software and Applications Conference, COMPSAC, Vol. 1, 2019, pp. 942–943, http://dx.doi.org/10.1109/COMPSAC.2019.00152.

[32] A. Chowdhury, D. Das, R.C. Cheung, M.H. Chowdhury, Hardware/software co-design of an ECG- PPG preprocessor: A qualitative & quantitative analysis, in: 2023 International Conference on Electrical, Computer and Communication Engineering, ECCE, 2023, pp. 1–6, http://dx.doi.org/10.1109/ECCE57851.2023.10101536.

[33] T. Sadad, S.A.C. Bukhari, A. Munir, A. Ghani, A.M. El-Sherbeeny, H.T. Rauf, Detection of cardiovascular disease based on PPG signals using machine learning with cloud computing, Comput. Intell. Neurosci. (2022) http://dx.doi.org/10.1155/2022/1672677.

[34] L. Evdochim, D. Dobrescu, S. Halichidis, L. Dobrescu, S. Stanciu, Hypertension detection based on photoplethysmography signal morphology and machine learning techniques, Appl. Sci. (Switzerland) 12 (16) (2022) http://dx.doi.org/10.3390/app12168380.

[35] M.T. Islam, I. Zabir, S.T. Ahamed, M.T. Yasar, C. Shahnaz, S.A. Fattah, A time-frequency domain approach of heart rate estimation from photoplethysmographic (PPG) signal, Biomed. Signal Process. Control 36 (2017) 146–154, http://dx.doi.org/10.1016/j.bspc.2017.03.020.

[36] Y. Kurylyak, F. Lamonaca, D. Grimaldi, A neural network-based method for continuous blood pressure estimation from a PPG signal, in: Conference Record - IEEE Instrumentation and Measurement Technology Conference, 2013, pp. 280–283, http://dx.doi.org/10.1109/I2MTC.2013.6555424.

[37] O. Schlesinger, N. Vigderhouse, D. Eytan, Y. Moshe, Blood pressure estimation from PPG signals using convolutional neural networks and siamese network, in: ICASSP 2020 - 2020 IEEE International Conference on Acoustics, Speech and Signal Processing, ICASSP, 2020, pp. 1135–1139, http://dx.doi.org/10.1109/ICASSP40776.2020.9053446.